Characterization of a supersonic flowfield using different laser based techniques

by

Uwe Brummund and Frithjof Scheel

German Aerospace Center, DLR Lampoldshausen

D-74239 Hardthausen a.K., Germany

ABSTRACT

An experimental study for supersonic ramjet (Scramjet) application has been performed in a model combustion chamber. The combustion chamber has a very flexible design and has been equipped with uv transmittive quartz windows from all four sides. Hydrogen fuel is injected with a Mach number of 2.0 parallel to the supersonic air flow (M=2.0). The non-reacting, compressible and turbulent flow has been studied using planar Rayleigh scattering and planar Mie scattering. The velocity distribution of the supersonic flow field has been determined by a Laser-Two-Focus technique (L2F). The shock and expansion waves have been visualized with high spatial and temporal resolution by the planar laser based techniques. Absolute shear layer thickness data based on the full width at half maximum criterion of the measured profiles have been determined from the visualized flow field. It is shown that planar Rayleigh scattering suffers considerably from low signal intensities especially at far downstream positions of the supersonic flow field. With the help of particle seeding methods using planar Mie scattering the intensity signal between regions of hydrogen and air has been much enhanced leading to high signal-to-noise ratios. The normalized shear/mixing layer growth rate has been determined in dependence of the convective Mach number M_c. With increasing compressibility level the normalized shear/mixing layer growth rate decreases which agree reasonably well with previous results by other experimenters. A shock wave generated at the inclined upper model combustion chamber wall interacts with the shear/mixing layer leading to enhanced spreading of the shear layer. It is shown that the normalized shear/mixing layer growth rate with shock impingement is only slightly higher than for the case without shock impingement.

1. INTRODUCTION

Air-breathing propulsion systems offer the potential of higher performance than rocket engines for hypersonic flight. A possible propulsion option is the supersonic combustion ramjet engine (scramjet). In such an engine, fuel-rich flow is mixed with a supersonic airstream. Combustion in supersonic flow is fundamentally different from combustion in the subsonic regime, i.e. ignition and flame stabilization processes known from the subsonic regime are not applicable to supersonic combustion devices. The success of future hypersonic propulsion systems will be largely dependent on efficient injection, mixing and combustion processes inside the supersonic/hypersonic combustion chamber. Therefore mixing and combustion efficiency in the supersonic flow regime is of great concern since the growth and entrainment rates of compressible shear layers are known to be much smaller than those of incompressible flows at the same velocity and density ratios. To improve the current understanding of the fundamental aspects of supersonic combustion it is desirable to perform non-reacting supersonic mixing studies as well as studies of the supersonic combustion process.

Experimental techniques frequently used in studying sonic and supersonic flows have been schlieren/shadowgraph flow visualization, pitot and concentration measurements. While these techniques gave valuable information about the flow field, they only yield point-by-point measurements and line-of-sight information, i.e. spatially integrated visualization possibilities.
Laser-based diagnostic techniques offer several advantages over these conventional methods for mixing and combustion studies owing to their nonintrusive nature and their capability for providing spatially and temporally resolved multipoint flow visualization. Planar laser Rayleigh and Mie scattering has been successfully employed for flow visualization in supersonic flows (Smith et al (1991), Hermanson (1993), Clemens (1991)). Planar Laser Induced Fluorescence (PLIF) is an especially attractive technique because it is both species and quantum state-specific (Bunyajitradulya (1994), Gross et al (1987)). Laser-induced iodine fluorescence has been used for temperature, density and velocity measurements in the flow field of non-reacting compressible jets (Fletcher (1989)). Laser-2-Focus (L2F) velocimetry is especially suited to measure the very high flow velocities in a scramjet combustion chamber (Schodl, 1986).

The principal objective of the research at DLR Lampoldshausen is to gain a more fundamental understanding of the flow physics and chemistry in compressible turbulent reacting and non-reacting flows. The project concentrates on two fundamental efforts: (1) an experimental study of mixing processes in non-reacting supersonic flows as well as combustion studies in reacting supersonic flows, and (2) development of laser based diagnostic techniques for time-resolved multi-dimensional imaging of species concentration, temperature, velocity and flow visualization in supersonic model combustion chambers.

2. EXPERIMENTAL METHOD

2.1 Experimental Facility

The test facility is a modular setup, consisting of a separate air heater producing vitiated air, a hydrogen support line equipped with an H_2/O_2 burner for heating up the hydrogen and a rectangular combustion model chamber.
The air can be heated up by a hydrogen/oxygen precombustion to maximum total temperatures of T_t=1500K at a maximum mass flow rate of 3 kg/s. Hydrogen can be heated up to maximum total temperatures of T_t=1100K with a maximum mass flow rate of 50 g/s.
The convective Mach number M_c has been changed by changing the total temperatures of hydrogen and air. The experimental parameters for all test conditions are listed in table 1.

	M_c = 0.8	M_c = 0.9	M_c = 1.0
gas_1,gas_2	H_2 ; air	H_2 ; air	H_2 ; air
M_1 ; M_2	2.0 ; 2.0	2.0 ; 2.0	2.0 ; 2.0
U_1 ; U_2 [m/s]	2090 ; 891	2090 ; 788	2090 ; 670
T_{t1} ; T_{t2} [K]	1100 ; 500	1100 ; 900	700 ; 500
P_{t1} ; P_{t2} [bar]	7.51 ; 7.62	7.51 ; 7.65	7.51 ; 7.52
$\dot{m}_1$; $\dot{m}_2$ [kg/s]	0.022 ; 1.07	0.022 ; 1.21	0.022 ; 1.41
$s = \rho_1/\rho_2$	5.66	7.08	9.64

$r = U_2/U_1$	0.427	0.381	0.326

Table 1: Experimental Parameters
M_c = Convective Machnumber, M_i = Machnumber (1=H_2, 2=air); U_i= mean axial velocity ; T_{ti} = total Temperature ; T = static Temperature ; p_{ti} = total pressure ; m_i = mass flow rate ; s = density ratio ; r = velocity ratio

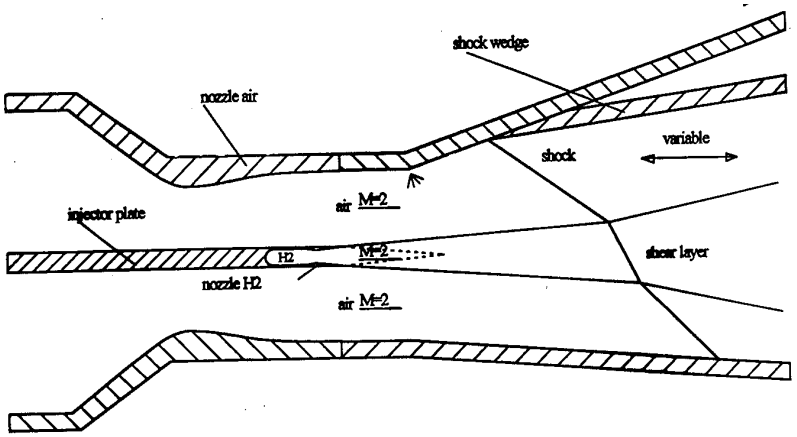

Fig. 1 Experimental supersonic model combustion chamber with plate injector
The scramjet model combustion chamber has a rectangular cross section of 40 mm x 50 mm and a length of 350 mm. For the non-reacting experiments a 6 mm thick plate injector located in the center of the chamber was used. At the base of this injection plate six bores in a row were manufactured as laval nozzles with a Mach number of M_{H2}=2.0. The leading edge of this injection plate is located upstream the laval nozzle of the air supply (Mach number M_{air}=2.0), so that no shock train can be initiated at this plate.
The shock waves itself were generated by a wedge plate located at the upper wall of the combustion chamber. The shock strength has been variied by changing the inclination angle of the shock generator (θ=7° and 15°). The position of the shock-mixing layer interaction was fixed to x=40mm in this study, whereas in former experiments applying the schlieren and pitot probe technique locations at x = 40mm, 60mm and 100mm have been chosen.
The combustion chamber was equipped with uv transmittive suprasil quartz windows from all four sides in order to allow full optical access. Typical test run times were 15 - 20s.

2.2 The Laser system

The laser system consists of a tunable narrowband excimer laser (Lambda Physik LPX 150T) which was used as the light source. It consits of an oscillator and amplifier part. The pulse length was about 17 ns which is essentially instantaneous to freeze the flow. The laser was operated at the KrF transitions working in the deep uv at 248 nm or at the ArF transitions at 193 nm. The laser energy measured directly behind the amplifier stage was typically 150-200 mJ per pulse. Spherical and cylindrical lenses were used to form the rectangular laser band into a thin sheet (0.3 mm thickness, 40 - 60 mm width) which was then directed into the centerline of the combustion chamber initiating the scattering process. The emitted light was detected under 90° by an intensified charge-coupled device (CCD) camera via a uv-light-sensitive lens (UV-Nikkor 105mm, f/4.5). The Flamestar camera system consists of an UV sensitive high gain image intensifier (S20 photocathode, P20 phosphor) fibroptically coupled with the CCD chip. The CCD chip has a resolution of 384 x 288 pixels, 12 bit per pixel. The intensifier was gated so that the camera records only 100ns after each laser pulse to suppress unwanted fluorescence. The resulting graysacle pictures were digitized, stored in a computer and presented in false colors on an online monitor. A personal computer with special acquisition software controlled the whole system, i.e., triggered the laser and the camera system via a timing unit and acquired the CCD images. The evaluation of the acquired CCD images was also possible with this software.

Fig 2. Experimental setup of the laser system

The velocity distribution within the supersonic combustion chamber has been measured by L2F, i.e. the laser-two-focus technique (L2F) (Schodl, 1986). This technique determines the velocity of extremely small particles which are often present in technical flows or may be added if required. The scattered light which the particles emit when irradiated by a light source is used in this method. In the measuring volume of the L2F-device, which was located 500mm from the optical system, two highly focused parallel laser beams are projected which operate as a light barrier. Each of the particles conveyed by the flow which pass through the two beams emit two consecutive light signals and the time interval serves as a measure for the determination of the particle velocity component perpendicular to the beam axis. Two associated signals are only then obtained when the plane through which the two beams are spread out is adjusted almost parallel to the flow direction. In turbulent flows the magnitude and direction of the momentary velocity vector changes permanently. Therefore the beam plane is adjusted by rotating some optical components of the device in various positions in the range of the mean flow direction and a preset number of time-of-flight measurements were carried out for each angular position. From the resulting 2-D histogram of successful particle transits mean flow quantities as magnitude and fluctuation level were determined.

2.3 Non-reacting Mixing layer studies

For the non-reacting mixing and mixing augmentation studies two different laser based techniques have been applied, i.e. planar Rayleigh scattering and Mie scattering.

Rayleigh Scattering

The Rayleigh Scattering technique is based on the fact that when a molecule interacts with an incident light beam, it extracts energy from the light wave and reemits this energy as a scattered light wave in all directions. The scattered light is at the same frequency as the incident light wave, indicating that Rayleigh scattering is an elastic process. It is also known that if the incident light wave is linearly polarized in the vertical plane, the

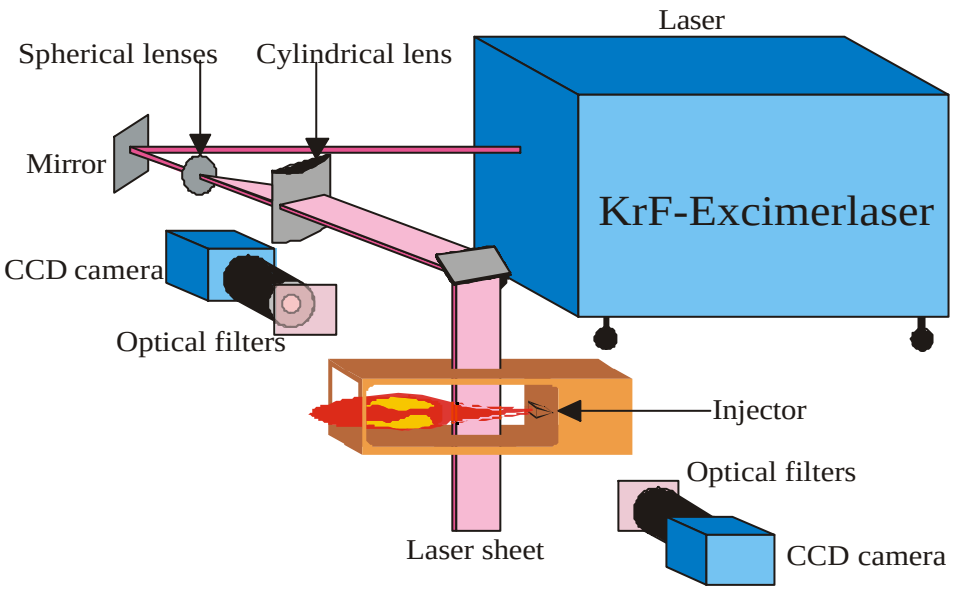

scattered light from the molecule will be at its maximum in the horizontal plane normal to the plane of polarization. The amount of light is usually expressed in terms of the scattered cross section of the molecule. Since the scattering cross section is different for each species, the scattered light will also be different enabling to visualize mixing processes of H_2 and air. For a mixture of two gases, the total scattering intensity is given as

$$I = P \cdot C \cdot N \cdot \Sigma X_j \cdot \sigma_j \qquad (1)$$

with (j=1 for H_2, j=2 for air), where X_j and σ_j are the mole fraction and the scattering cross section, respectively, of species j, P is the power of the incident light beam, and C is a constant of the optical system. In subsonic flows the unknown mole fractions X_j can be quantitatively determined after having used the system to calibrate the scattered intensity for each species. The implicit assumption is that the static pressure and the temperature is the same for all the measurements which is almost the case for incompresible or low-speed flows. In compressible flows especially in supersonic flows, there will be variations in pressure and temperature due to compression/expansion processes. This complicates the separation of the contribution from the two components. The pressure and temperature have not been measured up to now so the Rayleigh scattering images will be used as a qualitative measure for the density of air and H_2. Nevertheless the mixing layer thickness can be measured quantitatively from the measured Rayleigh images by profiling the images along the combustion chamber.
It is well known that the presence of water content in the air heater can have strong effect on the interpretation of Rayleigh images, even for very low water concentrations (ppm level). As the flow expands through the nozzle, the water molecules can agglomerate into very small ice clusters eventually dominating the Rayleigh signal. Due to this effect it was not possible to measure Rayleigh scattering images below static air temperatures of 300K.
Another problem applying Rayleigh Scattering is stray light reflected from windows and walls which can completely overshadow the molecular scattering signal. To prevent this unwanted signal intensity the laser beam was shielded. To reduce background light scattering, the test section walls were sprayed with black heat resistant colour.

Mie Scattering

A disadvantage of Rayleigh scattering is the decreasing intensity difference between regions of H_2 and air flows when intensive mixing between the two flow fields occur. An alternative to Rayleigh scattering for flow and mixing visualization is to take advantage of the large scattering cross sections of particles seeded into the flow. Detection of images and mixing layers far downstream the injector are now possible with good S/N ratios. Several different seed particles have been used in high speed wind tunnels, such as smoke, liquid droplets and solid particles and are discussed by Settles (1983). Different seeding methods have been employed depending on the flow conditions. These methods were the condensation seeding using alcohol droplets and suspended seeding using fine metal oxide powders.
In this study TiO_2 particles were used to seed the flow. The particles were first suspended inside a seeder and got transported into the hydrogen injector marking the H_2 flow field within the combustion chamber. The particle flow dynamics, i.e. the effects of inertia of a particle on its dispersion and its flow tracking capability is given by the Stokes number, which is the ratio of the characteristic particle τ_p to fluid time τ_f. The characteristic particle time is the amount of time it takes to stop a spherical particle of diameter D, density ρ and velocity u in aquiescent fluid. This time is given by $\tau_p = \rho \cdot D^2/18 \cdot \mu$, where μ is the viscosity of the fluid. The characteristic fluid time τ_f is given by the turn-over time in large eddies. In visualizing large-scale structures in the shear layer, the shear layer vorticity thickness and the velocity difference across the layer can be used to estimate the turn-over time. The maximum permissible Stokes number for correct visualization of large-scale turbulent structures is about 0.25 according to computations of Samimy (1990). For the present experiments TiO_2 particles were used with nominal diameters of 0.25 µm and 0.18 µm. For the 0.25 µm particles Stokes numbers in the range of 0.28 - 0.48 were estimated, whereas for the 0.18 µm particles the estimated Stokes number lie in the range of 0.11 - 0.23 in the order of increasing convective Mach numbers using the shear layer visible thickness. This estimation shows that one has to take care to choose the right size of the seeding particles. However, in this study the main aim of seeding the flow was to mark the mixing zone in order to calculate the mixing layer thickness, which has been done by analyzing the averaged Mie scattering images and not to resolve the details of the large scale structures. Due to this fact it can be concluded that it is possible to calculate the mixing layer thickness by the Mie scattering technique.

Compressible free shear / mixing layer

Shear layers are generated at the interface between the two streams of different velocities $u_1 > u_2$, in which momentum and vorticity is transported laterally from the faster to the slower stream. If thermal and mechanical energy as well as mass (molecules) are transported laterally and the two streams have different molecular identities (as is the case for air and H_2), the shear layer is also a mixing layer. The mixing layer thickness δ_m is defined as the region within which the mole fractions of air and fuel differ by one percent or more from their respective values in the unmixed streams. It is known that the time-averaged mixing layer is observed to grow approximately as a constant fraction of the shear layer in the fully developed region of the shear layer (Heiser, 1994). Nevertheless, it has to keep in mind that there are many different ways the shear layer thickness has been defined in literature, i.e. the visual shear layer thickness δ, the 10%ΔU thickness, the pitot thickness, the

momentum layer thickness θ, and the vorticity thickness δ_ω. In this study the visual shear layer thickness δ_{vis} defined as the full width at half maximum (FWHM) of the cross sections of the Rayleigh and Mie scattering images was used. The most well-known effect of compressibility on shear layers is the reduction of the growth rate $d\delta/dx$ that occurs as compared to that of incompressible layers at the same velocity and density ratios. The reduced growth rate was thought to be due to the density difference between the streams that occur under compressible flow conditions. It was shown that the density effect was small and that the growth rate reduction must be due to a separate and stronger compressibility effect (Samimy, 1990). This compressibility effect is quantified by the convective Mach number M_c which is the Mach number of the two freestreams relative to the large scale structures in the mixing layer

$$M_c = \frac{U_1 - U_2}{a_1 + a_2}, \qquad (2)$$

where u_i (i = 1,2) is the freestream velocity of air and H_2 and a_j (j=1,2) is the speed of sound of air and H_2, respectively.
For comparison with data from literature the growth rate $(d\delta/dx)_{com}$ of the compressible shear/mixing layer has been normalized using the incompressible growth rate

$$\left(\frac{d\delta}{dx}\right)_{inc} = C_\delta \cdot \frac{(1-r)\cdot(1+r)}{1+r\cdot\sqrt{s}}, \qquad (3)$$

with $s=\rho_2/\rho_1$ and $r=U_2/U_1$ and C_δ = 0.17 as a constant for pitot and schlieren flow visualization. The decreasing mixing layer growth rate is in contradiction to the aim of a fast and effective mixing in supersonic flows. One possibility to enhance this growth rate is the interaction of a shock wave with the mixing layer. This study has been done by varying important parameters like the shock strength (by variation of the upper wall angle) and the convective Mach number M_c by varying the temperature of H_2 and air, respectively in order to perform a parametric study of the influence of these parameters on the growth rate enhancement.

3. RESULTS AND DISCUSSION

3.1 Mixing layer development and similarity profile

For a mixing layer to be considered fully developed, it is required that both the mean and turbulent velocity fields be self similar. Generally, the mean velocity field requires less streamwise distance to become self similar with increased development lengths being required for the streamwise turbulence intensity, transverse turbulence intensity, and Reynolds stress, respectively. Estimates of the lengths required for development of the streamwise mean velocity have been determined from the L2F measurements.
The requirements for full development of incompressible mixing layers have been studied by Bradshaw (1966). For a single stream shear layer, Bradshaw found that full development, in terms of Reynolds stress, required a Reynolds number based on streamwise distance $Re_x=\rho\cdot U\cdot x/\mu$ of approximately $7\cdot10^5$, where ρ is the density, U the local mean streamwise velocity, μ the viscosity and x the streamwise coordinate. The initial thickness of the boundary layers had very little effect, whether they were laminar or turbulent.
An appropriate translation of this Reynolds number for application to compressible two stream mixing layers would be based upon the freestream velocity difference ΔU, the local mixing layer thickness s, and the average freestream properties. The development criterion would then be a local Reynolds number with a value of approximately $Re_s=\langle\rho\rangle\cdot\Delta U\cdot s/\langle\mu\rangle = 1\cdot10^5$, where $\langle\rho\rangle$ is the ensemble averaged density, ΔU the freestream velocity difference U_1-U_2, s the mixing layer thickness, and $\langle\mu\rangle$ the averaged viscosity. This local Reynolds number has been estimated for each of the studied cases and this modified criterion seems to hold for the development of the compressible mixing layers presented here.
Once a mixing layer has become fully developed, the velocity profiles can be expressed in self-similar form. The regions of the mixing layers where the mean streamwise velocity was considered to be self similar and that were used to determine the mixing layer growth rates have been estimated to be $x \geq 60$mm (see Fig. 3). Generally only thickness data from the region where the mean streamwise velocity was self similar were used to determine the growth rates.

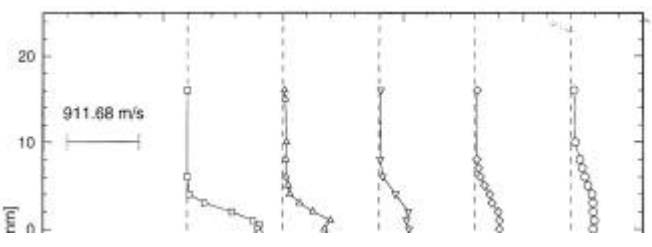

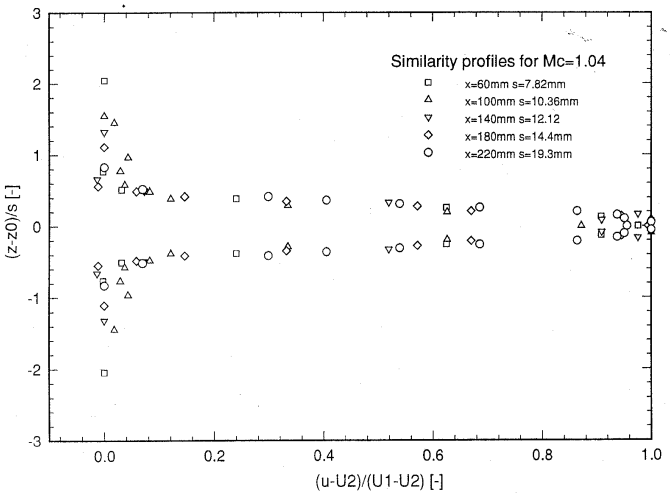

Fig. 3 Axial mean velocity profile and corresponding similarity profile for M_c=1.04

3.2 Rayleigh and Mie scattering imaging

A typical averaged Rayleigh scattering image of the supersonic flow field without shock impingement and a convective Mach number of M_c=1.0 is shown in figure 4 (x = 0 - 35 mm) . The image is presented using a gray scale, where white corresponds to the lowest recorded scattering intensity, all images have been corrected for laser sheet inhomogenities and stray light reflections. The flow direction is from left to right. The system of expansion waves as well as the central part of the mixing layer is readily revealed by the averaged Rayleigh scattering image (20 laser shots).

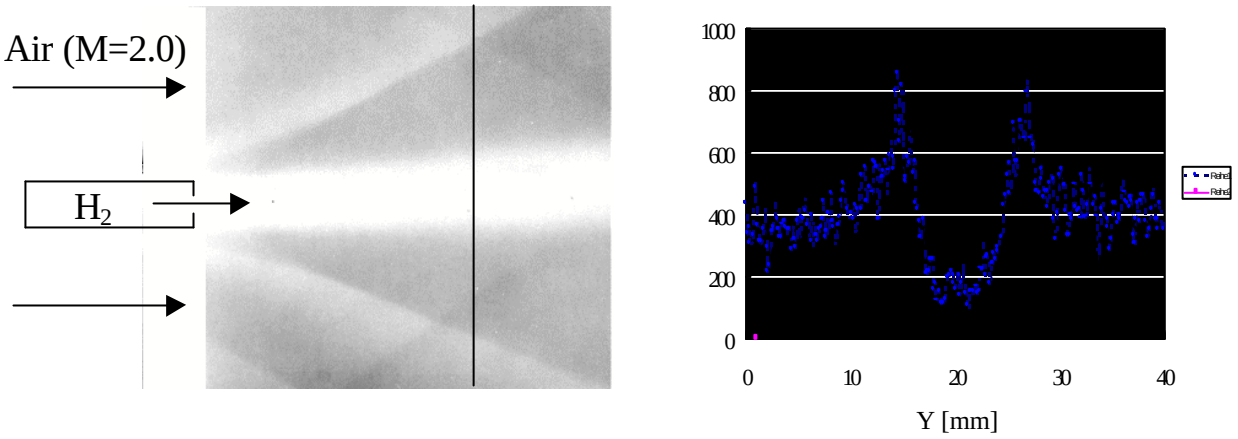

Figure 4: Averaged Rayleigh scattering image of the mixing layer zone in the vicinity of the plate injecotr and corresponding intensity profile

The mixing layer thickness has been determined from such images by taking a cross section along a vertical line of the picture, resulting in an intensity profile.The mixing layer thickness δ_m has then been defined as the full

width at half maximum (FWHM) of this intensity profile. The mixing layer growth rate $d\delta/dx$ has been determined by analyzing 15-20 of such intensity profiles downstream the injection plate, resulting into a linear curve which has been fitted with a least square fit algorithm. Finally this growth rate of the compressible mixing layer has been referenced with the incompressible mixing layer growth rate (equation 3), resulting in the normalized mixing layer growth rate δ_c'/δ'_{inc}, which has been used in order to compare our data with data from literature.
A severe problem of using Rayleigh scattering is that downstream the injector enhanced mixing leads to very low intensity differences between regions of air and hydrogen. At downstream locations x > 140 mm this reduced intensity difference complicated the determination of the mixing layer thickness from planar Rayleigh scattering images very much.
To overcome this problem and in order to get much higher signal intensities, the Mie scattering technique, was applied forcing to use seed particles. A typical averaged Mie scattering image is seen in figure 5.

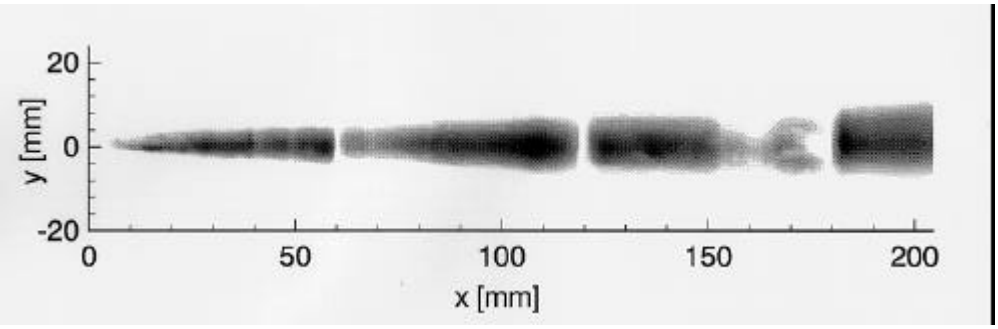

Fig 5: Averaged Mie scattering image of the mixing layer zone wiothout shock impingement

The image is a composite obtained at different downstream locations and acquired at different test runs. The image is also represented by using a gray scale, black corresponds to the highest recorded scattering intensity and the same image correction procedure has been performed as with the Rayleigh scattering images. 20 laser shots have been averaged for this Mie scattering image of the supersonic H_2/air mixing layer without shock-mixing layer interaction.
As can be seen the mixing layer can be visualized with high signal intensity and is spreading along the combustion chamber. Furthermore it was possible to image the whole mixing layer along the combustion chamber length. The reduced signal at x = 160 - 180 mm is probably due to insufficient seeding of the TiO_2 particles density. The images presented here demonstrate the applicability of the Mie scattering technique for visualizing supersonic mixing layers. Important advantages of this diagnostic technique vs Rayleigh scattering include a relatively high signal strength. Although the Mie scattering technique can be employed easily to obtain useful information on turbulent structure and growth rate, the technique does not directly provide quantitative information on the amount of dilution or mixing. Estimation of these quantities requires separate information of the particle sizes and number densities. This information is not unambigiously provided by Mie scattering, as the signal strength is proportional to the product of the particle number density and the scattering cross section. To obtain quantitative estimates would thus require some understanding of the nucleation process, which in turn necessitates knowledge of the temperature field, but was beyound the scope of this work.

Effect of compressibility on the mixing layer

In order to compare the data of this work with data from literature the normalized mixing layer growth rate δ_c'/δ'_{inc} has been plotted in dependence of the convective Mach number M_c as seen in figure 6.

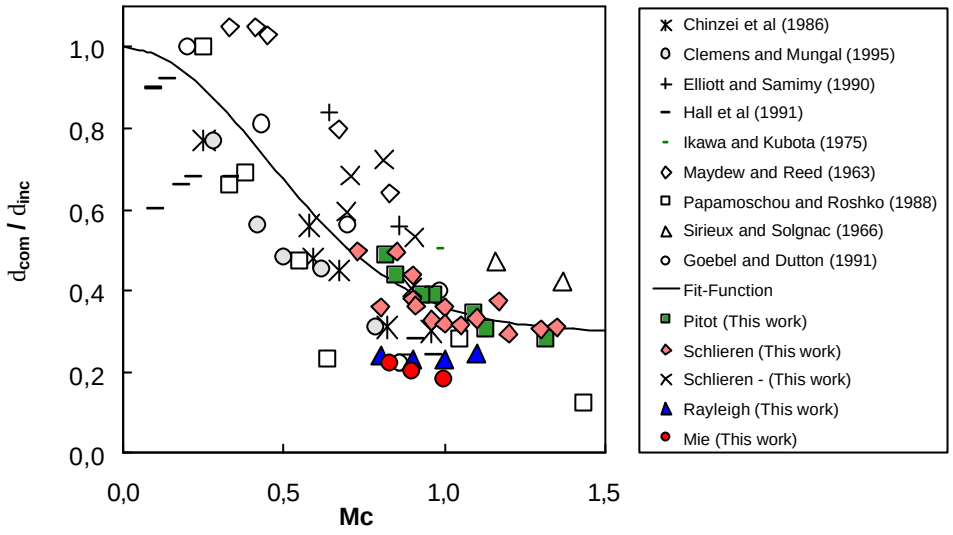

Fig 6: Normalized mixing layer growth rate in dependence of the convective Mach number M_c

For the laser based measurements the convective Mach number range was limited to M_c=0.8-1.0 due to condensation effects in the combustion chamber. From former experiments using pitot probe and schlieren measurements a fit function to all of the experimental data points has been derived represented by the following equation:

$$\delta'_{com} / \delta'_{inc} = 0.7 \cdot e^{-2.5 M_c^2} + 0.3 \qquad (4)$$

This relation represents the compressibility effect on the mixing layer growth rate and is also used as a reference for the mixing layer studies with shock interaction. The solid line in figure 6 represents this fit. As can be seen the mixing layer growth rate is a decreasing function as the compressibility represented by the convective Mach number M_c increases. This result is in good agreement with results from literature (Bogdanoff, 1983, Chinzei, 1986, Samimy, 1990, Clemens, 1990) and confirms that our supersonic mixing layer setup works quite well.
The Rayleigh and Mie scattering results have also been included in figure 6. As can be seen the values of the normalized mixing layer growth rates measured by the laser optical diagnostic techniques are all a little bit lower than the pitot and schlieren measurements. At first glance this is a surprising result because one should guess that the mixing layer has a defined thickness independent of the applied measurement technique.
Possible reasons for this discrepency may be due to differences in the thickness definitions mentioned above and in the shear/mixing layer definition. With schlieren measurements the shear/mixing layer thickness was always determined „by eye“ which is somewhat subjective. The outermost edge of the shear layer of each schlieren picture has been taken as a measure for the shear layer thickness. Of course this estimation results in relatively thick shear layers. For the laser based diagnostic techniques the shear layer thickness has been defined as the full width at half maximum (FWHM) value which delivers smaller values for the mixing layer thickness and even smaller ones made by the Mie scattering technique. This effect can be explained by the fact that for Mie scattering only the hydrogen is seeded and thereby marked by the TiO_2 particles. Estimation of the FWHM thickness delivers the smallest values and is actually a measure of the mixing layer. In a very simplified way it can be stated that the actual shear layer thickness is best measured by the schlieren technique, the mixing layer thickness is measured by the Mie scattering technique and the Rayleigh scattering technique delivers values laying in between these two measured values. It therefore turns out that one has precisely to distinguish between the mixing layer thickness δ_m and the shear layer thickness δ.

Shock-wave -induced mixing enhancement

Figure 7 shows a composite Mie scattering image of the mixing layer interacting with a shock wave reflected at the upper chamber wall which was inclined by 15° (convective Mach number M_c=0.9). The inclined upper wall (shock generator) and the reflected shock are schematically indicated by the solid and dashed lines in figure 7. The image clearly reveals the influence of the shock wave on the mixing layer. It can be recognized that the mixing layer is deflected due to the shock impingement. Furthermore the mixing layer seems to be spread a little

bit more after the shock impingement. Instantaneous Rayleigh images give good insight into the details of the shock mixing layer interaction process. Single shot planar Rayleigh scattering measurements have been performed showing that the reflected shock wave initiates vortices, rolling up the mixing layer and thereby enhancing the spreading of the mixing layer. The visual mixing layer thickness has been measured for three different test cases (M_c=0.8, 0.9 and 1.0) by variation of the wedge angle of the shock generator (7° and 15°) and a fixed shock-mixing layer interaction region located at x=40mm.

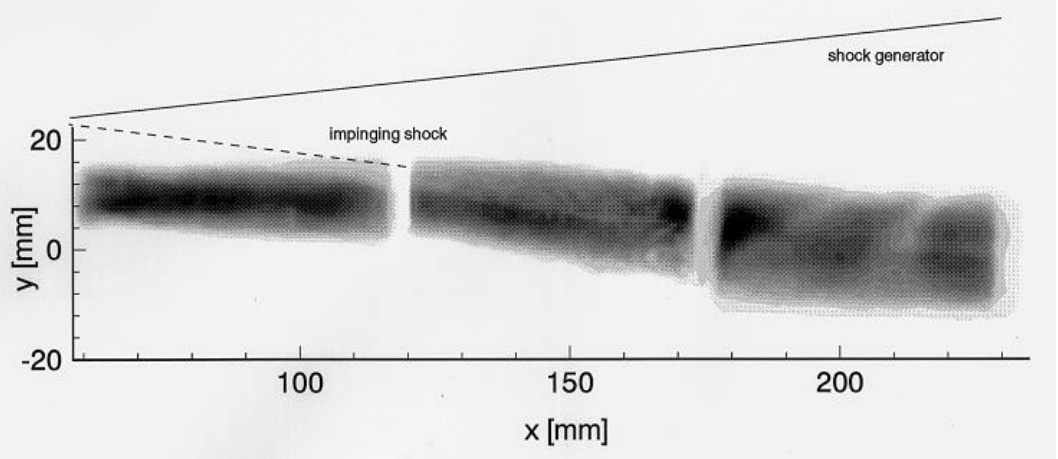

Fig 7: Mie scattering image of the mixing layer zone with shock impingement

In figure 8 the normalized mixing layer growth rate with shock interaction of a 7° wedge angle is shown together with the fitted curve of equation (8). It can be seen that all measurement points lay above this fitted curve which serves as a reference for the non-shock/shear layer interaction case. The experimental results for the 15° wedge angle indicate the same trend (not shown here).

Fig 8: Normalized mixing layer growth rate with shock impingement for a wedge angle of 7° Tough there is some data scatter and only a very limited range of convective Mach numbers M_c have been measured the results seem to indicate a slight, but significant enhancement of the normalized mixing layer growth rate by a shock-mixing layer interaction. The shock wave-mixing layer interaction is therefore a suitable means to improve the mixing process in compressible flows.

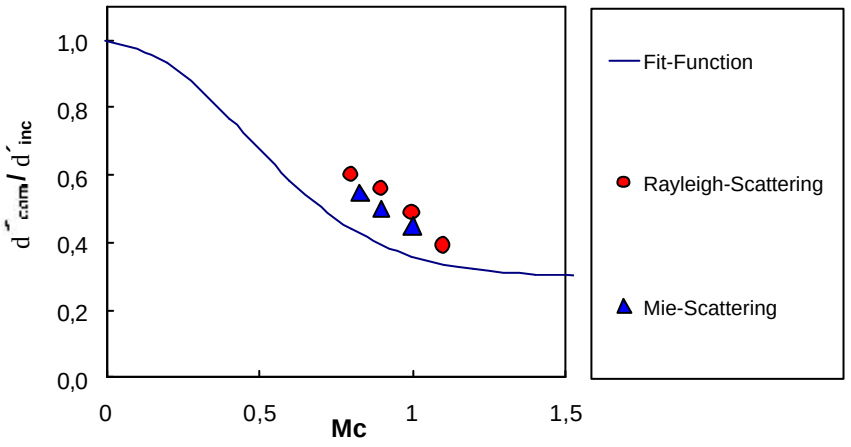

Fig. 8: Normalized mixing layer growth rate with shock impingement (θ = 7°)

4. SUMMARY

An experimental investigation has been performed in a non-reacting M=2.0 supersonic combustion chamber in order to study the behavior of compressible mixing layers in high speed flows. The velocity distribution has been characterized by L2F technique. The visual mixing layer thickness has been measured by laser-based optical diagnostics (Rayleigh and Mie scattering). The compressibility, expressed by the convective Mach M_c has been variied by changing the H_2 and air temperatures from M_c = 0.8 - 1.0 in order to study the compressibility influence on the shear/mixing layer growth rate. The study shows that the normalized mixing layer growth rate is decreasing with increasing compressibility, expressed by the convective Mach number M_c. This result is in good agreement with data from literature. In order to find possible ways for enhancing the mixing layer growth rate shock-induced shear/mixing layer experiments have been performed. It has been shown that there is a slight, but significant enhancement of the normalized mixing layer growth rate depending on the shock strength and the location of the interaction region.

REFERENCES

Bogdanoff, D.W. (1983). "Compressibility Effects in turbulent Shear Layers," AIAA Journal, Vol. 21, No.6, pp. 926-927.

Bradshaw, P. (1966). "The Effects of Initial Conditions on the Development of a Free Shear Layer," Journal of Fluid Mechanics, Vol 26, pp. 225-236.

Bunyajitradulya A., Papamoschou D. (1994). "Acetone PLIF Imaging of turbulent Shear-Layer Structure at high Convective Mach Number", AIAA-Paper No. 94-0617.

Chinzei, N.,Masuya, G., Komura, T., Murakami, A., and Kudou, K. (1986). "Spreading of Two-Stream Supersonic Turbulent Mixing Layers", Physics of Fluids, Vol. 29, pp. 1345-1347.

Clemens, N. T., Mungal, M. G. Berger, T. E. and Vandsburger, U. (1990). "Visualization of the structure of the turbulent mixing layer under compressible conditions", AIAA Paper 90-1978, 1990.

Clemens N.T., Mungal M. G. (1991). "A planar Mie scattering technique for visualizing supersonic mixing flows", Exp. Fluids, 11, pp. 175-185.

Fletcher D.G., McDaniel, J.C. (1989). "Laser Induced Iodine Fluorescence Technique for Quantitative Measurement in a Nonreacting Supersonic Combustor," AIAA Journal, Vol. 27, No.5.

Gross, K.P.,McKenzie, R.L.,Logan, P. (1987). "Simultaneous Measurements of Temperature, Density, and Pressure in supersonic Turbulence Using Laser-Induced Fluorescence". Exp.Fluids, Vol. 5.

Heiser, W.H., Pratt, D.T. (1994). "Hypersonic Airbreathing Propulsion", AIAA Education Series, American Institute of Aeronautics and Astronautics, Wahington, DC.

Hermanson, J.C. and Winter M. (1993). "Imaging of a transverse, sonic jet in supersonic flow", AIAA Journal, Vol. 31, No.1.

Samimy, M., Lele, S.K. (1990). "Particle-Laden Compressible Free Shear Layers", AIAA Paper No. 90-1977, 26th Joint Propulsion Conference, Orlando, FL.

Samimy, M., Elliot, G.S. (1990). "Effects of Compressibility on the Characteristics of Free Shear Layers", AIAA Journal, Vol. 28, No. 3.

Smith, D.R., Poggie, J., Konrad, W., Smiths, A. J., (1991). "Visualization of the structure of shock wave turbulent boundary layer interactions using Rayleigh scattering", AIAA Paper 91-0460.

Settles, G. S., Teng, H. Y. (1983). "Flow Visualization Methods for Separated Three-Dimensional Shock-Wave/Boundary Layer Interactions", AIAA Journal 21, pp. 390-397.

Schodl, R. (1986). "Laser-Two-Focus velocimetry", Advanced Aero Engine Components, AGARD-CP-399, p.7, Philadelphia.